




Ultrastable laser referenced on velocity-grating atom interferometryHaosen Shang ^{1,*}, Duo Pan,^{1,*}† Xiaogang Zhang,¹ Xiaobo Xue ², Tiantian Shi,¹ and Jingbiao Chen ¹¹State Key Laboratory of Advanced Optical Communication Systems and Networks, Department of Electronics, Peking University, Beijing 100871, China²Science and Technology on Metrology and Calibration Laboratory, Beijing Institute of Radio Metrology and Measurement, Beijing 100854, China

(Received 29 August 2021; accepted 2 May 2022; published 23 May 2022)

A laser with superb frequency stability plays an important role in fundamental physics research and advanced technologies. Frequency references are usually utilized to stabilize the laser, such as high-finesse cavities and atomic ensembles, of which thermal atomic beams are attractive because of their balanced performance between simplicity and stability. However, due to the transverse-velocity distribution in the thermal atomic beams, most atoms (generally >99%) are wasted when interacting with the laser. Here, we propose a laser referenced on a version of velocity-grating Ramsey-Bordé atom interferometry with greatly improved atom utilization and thus superior laser frequency stability. Compared with a conventional atomic interferometry applied to stabilize the laser, the proposed system in principle generates optical Ramsey fringes with the amplitude enhanced by 1000-fold or more. Such a configuration has promising applications in diverse areas, including precision measurements and quantum metrology.

DOI: [10.1103/PhysRevA.105.L051101](https://doi.org/10.1103/PhysRevA.105.L051101)

A laser with outstanding frequency stability has undergone significant progress in fundamental physics research and advanced technological applications. The latest developments, e.g., gravitational wave detection [1] and ultralow phase noise microwave sources [2,3], reveal its great potential to break through the boundaries of traditional methods. One inspiring application is the optical clock [4–6], which enables the frequency measurement to reach an unprecedented level of precision, i.e., 10^{-19} [7,8]. Such an ability of optical clocks promotes fields in the generation of timescales defined in the optical regime [9,10], tests of general relativity [11,12], and monitoring of geopotentials [13,14] based on clock networks [15].

Recent efforts [16–18] have promoted the performance of frequency-stabilized lasers referenced on the cryogenic Si cavity to reach a thermal noise-limited instability of 4×10^{-17} [8]. A more stable laser requires lower thermal cavity noise, and subsequently more technical challenges [16,17], thus motivating the research on alternative approaches, including spectral hole burning [19] and active optical clocks (superradiant lasers) [20–24]. Considering the remarkable resolution and signal-to-noise ratio (S/N) contributed from numerous atoms, thermal atomic ensemble-based Ramsey-Bordé atomic interferometry is an eminent choice for laser frequency stabilization, with a short-term instability of 10^{-16} [25] already presented, as well as superior long-term stability and accuracy over reference cavities. As in prior studies, owing to the pivotal application of spatially separated electronic-shelving

detection [26], thermal calcium beam atomic interferometry-based laser stabilization initially showed impactful frequency stability [27]. Subsequently, the frequency instability of the laser was further reduced to the level of 10^{-15} with Rabi excitation [28]. Recently, such an approach impressively demonstrated a frequency instability of $6 \times 10^{-16}/\sqrt{\tau}$ in short timescales [25,29]. However, the Ramsey (or Rabi) excitation in thermal beams generally encounters challenges in taking full advantage of atoms with nonzero transverse velocities [25–29]. Undoubtedly, only a fraction of atoms (<1%) among the large transverse-velocity distribution contribute to S/N , wasting nearly a trillion atomic references.

To address this problem, in this Letter we propose an ultrastable laser referenced on a version of velocity-grating Ramsey-Bordé atom interferometry relying on the accumulated contributions from an abundance of nonzero-transverse-velocity atoms in thermal atomic ensembles. The proposed system can dramatically enhance the amplitude of the optical Ramsey fringes by 1000 times, and thus promote laser stabilization with thermal atomic ensembles to a quantum projection noise (QPN)-limited frequency instability of $2 \times 10^{-17}/\sqrt{\tau}$ or less, which surpasses prior thermal atomic ensemble-based systems by more than one order of magnitude and is comparable with the best-reported optical clocks [8] in short timescales. Such a system opens a door for applications of thermal atomic ensembles in metrology and astronomy, by avoiding the ever-present trade-offs between system simplicity and measurement precision. Although Ca is used as an example here, the scheme is universal for different thermal atomic ensembles.

The experimental configuration of the laser referenced on the velocity-grating Ramsey-Bordé atom interferometry is illustrated in Fig. 1(a), wherein four $\pi/2$ lasers repeatedly

*These authors contributed equally to this work.

†panduo@pku.edu.cn

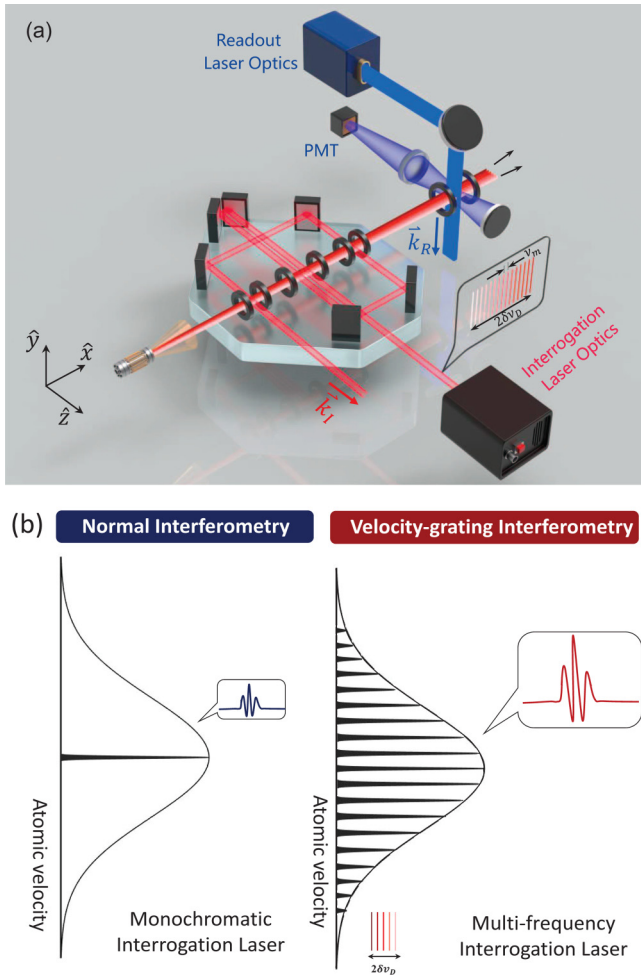


FIG. 1. (a) Scheme of the laser reference on the velocity-grating optical Ramsey atomic interferometry. Both the optical local oscillator (OLO) laser and readout laser are prestabilized. The OLO laser is phase modulated with a frequency of ν_m to be a multifrequency laser (interrogation laser) by a series of cascade phase modulators. The spectrum of the interrogation laser with a span of $2\delta\nu_D$ is shown in the black frame. The gradual colors in the atomic beam denote the atoms with different Doppler shifts. PMT: photomultiplier tube. \vec{k}_I and \vec{k}_R denote the wave vector of the interrogation laser and readout laser, respectively. Magnetic fields in the interrogation and readout zones are produced by four pairs of black coils. (b) The transverse-velocity distribution of atoms utilized in normal atom interferometry (left) and the proposed velocity-grating atom interferometry (right). For the normal case only atoms with near-zero transverse velocities contribute to the optical Ramsey fringe, while in the velocity-grating atom interferometry, atoms with equal transverse-velocity intervals can be interrogated and comprise a gratinglike distribution in the transverse-velocity domain.

interrogate the atomic beam. The quantum absorbers used here are neutral calcium atoms, possessing the $^1S_0 - ^3P_1$ transition (657 nm, ~ 400 Hz linewidth) insensitive to external field perturbations. For the directional atoms effusing from the oven heated to 625°C , the unavoidable transverse divergence would lead to a Doppler shift relevant to velocity along the \hat{z} direction. One typical method to suppress the adverse Doppler effect, namely a slit placed behind the oven nozzle, is usually

implemented at the cost of the great reduction of quantum absorbers. However, in the configuration proposed here, the downstream slit is not needed, so then a Doppler width can be typically up to 100 MHz [30,31].

An optical local oscillator (OLO, with an expected local Hz-level linewidth) is obtained after the 657-nm laser [pre-stabilized by an ultralow-expansion (ULE) cavity [25,29]] passes through an acousto-optic modulator (AOM), which is used to make up the frequency difference between the cavity and atoms. Before interacting with the calcium atoms, the OLO is phase modulated to be a multifrequency interrogation laser that has numerous narrow-linewidth sidebands. Any adjacent sidebands with equal intensities are separated by the modulation frequency ν_m , and each sideband keeps the spectral purity and phase coherence. The total number of spectral lines (NSLs) of the interrogation laser is $(2j + 1)$, and j is the modulation order. To maintain a uniform intensity distribution for each sideband and thus ensure an identical Rabi frequency for atoms with different transverse velocities, a practical technique, e.g., “flattop” electro-optic comb technology [32–35], can be introduced to the phase modulation process. Since the fully structured interferometry based on ULE glass spacers has been studied in detail [29], in the proposed scheme such a vibration-tolerable configuration is similarly adopted, where the length of the Ramsey free-evolution zone is set to ~ 9 cm (hence, the interrogation time is about 0.3 ms for calcium), and the distance between the two central fields is ~ 1 cm. A magnetic field (typically 5–7 G) is applied to pick the field-insensitive 3P_1 ($m_J = 0$) sublevel.

As an essential part of the configuration, a spatially separated readout laser corresponding to a fast transition is introduced to measure the population variation of the clock state. For calcium, either a 423-nm transition ($^1S_0 - ^1P_1$) or 431-nm transition ($^3P_1 - ^3P_0$) is the appropriate candidate [25,28] used here. Choosing the 431-nm laser can basically eliminate the noise induced by the unexcited ground-state atoms [28]; nevertheless, the 431-nm laser must be obtained from frequency doubling and is unable to be directly locked onto the $^3P_1 - ^3P_0$ transition of calcium [25,29,36]. The polarization of the readout laser is adjusted to be along the \hat{x} direction to maximize the intensity of the fluorescence, which is collected by the photomultiplier tube. Frequency corrections generated from the readout fluorescence are fed back to the AOM. To mitigate the influence of ac acceleration (i.e., vibrations) on the visibility of fringes, some strategies can be adopted, such as shortening the laser paths, using ULE materials as the baseplate for the mirrors, placing the mirrors into the vacuum chamber to reduce the influence of the airflow, and mounting the apparatus on a vibration-isolation table.

The line shape of the fluorescence acquired here is different from that of traditional Ramsey spectroscopy. For the case of using a multifrequency interrogation laser, the interrogated atoms are presented as a gratinglike distribution in the transverse-velocity domain [along the \hat{z} direction, shown in Fig. 1(b)], with each grid generating a Ramsey fringe and contributing to the detected central fringe. Compared with the traditional interferometer where only atoms with near-zero transverse velocities are kept but the atoms with large transverse velocities are filtered by the slit, the pro-

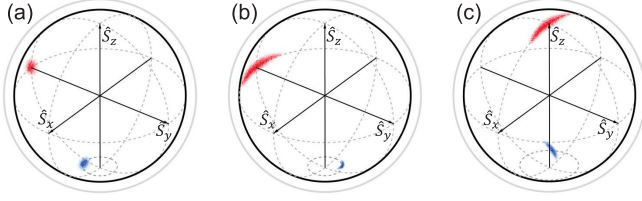


FIG. 2. Evolution of the pseudospin vector in the Bloch sphere for atoms with large transverse velocities in the case of a single-frequency laser (lower blue points) and multifrequency laser (upper red points). (a) After the first interrogation field. (b) After free evolution. (c) After the second interrogation field.

posed velocity-grating interferometer allows for a significant increase in signal-to-noise ratio without degrading the contrast of the spectroscopic interference fringes. The specific characteristics are analyzed and discussed below.

The complicated evolution processes of the atomic state in the optical Ramsey excitation especially for the multifrequency case will be explained below with the aid of the pseudospin picture. To simplify the explanation of the difference between our scheme and the traditional optical Ramsey method, only the evolution of the atomic state after the excitation of the first two fields is taken into account in the pseudospin picture here (see Fig. 2), owing to the fact that the two additional traveling fields in the optical Ramsey interferometer are merely used to rephase [29,37]. The atomic state denoted by the pseudospin vector in the Bloch sphere varies under the action of the “torque” vector $\vec{\Omega}$. Considering the Doppler effect, the vector can be expressed as $\vec{\Omega} = (-\Omega_R, 0, kv_z - \Delta)$, where Ω_R is the Rabi frequency, k is the wave vector of the field, v_z is the velocity of the atom along the \hat{z} direction, Δ is the frequency detuning of the carrier of the multifrequency laser to the atomic resonance, and the last term of the $\vec{\Omega}$ represents the frequency detuning. In the traditional single-frequency case, for a particular class of atoms with large transverse velocities $v_z \pm \delta v_z/2$ ($\delta v_z < 0.3$ mm/s), the vector $\vec{\Omega}$ is near the \hat{z} axis because $|kv_z| \gg \Omega_R$ (when the $\Delta \approx 0$). The pseudospin vector initially located at the south pole is rotated after the first interrogation field; see the lower blue points in Fig. 2(a). Experiencing a dark time of $\sim 10^{-4}$ s, the vector fans out since the $k\delta v_z$ is still significant in the optical regime despite the small δv_z . From the blue points in Fig. 2(c), it can be seen that the state vectors still distribute over the southern hemisphere under the excitation of the subsequent $\pi/2$ laser field, showing low transition probabilities for the atoms with large transverse velocities.

But when the OLO with a frequency of ν_L is modulated to be the multifrequency interrogation laser with frequencies of $(\nu_L \pm j\nu_m)$, namely in the case of a multifrequency interrogation laser, a class of atoms with velocity v_z satisfying $kv_z \simeq 2\pi p\nu_m$ (the integer $p \leq j$) must exist. When $\Delta \approx 0$, for such a class of atoms interacting with the $+p$ th sideband of the first two multifrequency laser fields with a frequency of $(\nu_L + p\nu_m)$, the vector $\vec{\Omega} = [-\Omega_R, 0, kv_z - (\Delta + 2\pi p\nu_m)] = (-\Omega_R, 0, -\Delta)$, which is the same as that of the zero-transverse-velocity atoms. Moreover, for the last two multifrequency interrogation laser fields, the sign of the wave

vector k is opposite, and then such a class of atoms can be excited by the $-p$ th sideband with a frequency of $(\nu_L - p\nu_m)$, leading to $\vec{\Omega} = (-\Omega_R, 0, -\Delta)$ as well. Concretely, the evolutions of the atomic state for atoms with a transverse velocity of $v_z \pm \delta v_z/2$ in this proposed configuration are given; see the red points in Figs. 2(a)–2(c), similar to the evolution processes of the atoms with near-zero transverse velocities [37]. Therefore, it can be found that almost all atoms with transverse velocity $v_z = 2\pi p\nu_m/k$ ($p \leq j$) can now be interrogated. These atoms comprise a gratinglike distribution in the transverse-velocity domain. Different from the traditional optical Ramsey method, the proposed method can make the most of the atoms with nonzero transverse velocities producing fringes, and thus the velocity-grating Ramsey fringes can be seen as the superposition of thousands of traditional Ramsey fringes in the frequency domain.

Considering the recoil effect but ignoring the relaxation of the state, the transition probability of one particular atom in the case of a single-frequency interrogation laser is given by [37]

$$P_e \propto \text{Re}\{K \exp[i2(\Delta \pm \delta)T + \phi]\}, \quad (1)$$

where K is related to the frequency detuning and Rabi frequency, Δ is the laser frequency detuning, δ is the photon recoil frequency, T is the free-evolution time, and ϕ the phase difference of the four laser fields. When the laser is modulated to be a multifrequency one, the electric field of which can be written as $\epsilon = \text{Re}\{E_0 \sum_{p=-j}^j \exp[i(\omega_L t + p\omega_m t - kv_z t + \varphi_i)]\}$, where E_0 is the amplitude of the sideband, and φ_i is the phase of each traveling field with $\phi = -\varphi_1 + \varphi_2 - \varphi_3 + \varphi_4$. Following the representation methods in Ref. [37], the Schrödinger equation is given as

$$i\hbar \frac{\partial}{\partial t} \begin{bmatrix} b_{l\pm 1} \\ a_l \end{bmatrix} = (E_{a(b)} + l^2 \hbar \delta + \hbar \Omega_R \epsilon / E_0) \begin{bmatrix} b_{l\pm 1} \\ a_l \end{bmatrix}, \quad (2)$$

where $|a_l|^2$ and $|b_l|^2$ are the transition probabilities of the ground state and excited state, respectively, l is the number of momentum quanta of atoms exchanged with the fields, $E_{a(b)}$ are the energies of the state, and $\hbar \delta$ is the photon recoil energy. Consider one particular sideband and class of transverse-velocity atoms which satisfies $p\omega_m \simeq kv_z$, assuming that other sidebands are “blind” to v_z atoms (that means v_z atoms cannot be excited by other sidebands by choosing a large ω_m). Solving Eq. (2) and obtaining the transition probability of the excited state for the multifrequency case, which is

$$P_e \propto \text{Re}\{K \exp[i2(\Delta \pm \delta)T + \phi]\} + O\{\exp[i(\mp p\omega_m \pm kv_z)T], \exp[i2(\mp p\omega_m \pm kv_z)T]\}, \quad (3)$$

this equation has the identical form to Eq. (1) since the last term in Eq. (3) can be neglected. This result is not unexpected and is consistent with the interpretation based on the pseudospin picture displayed in Fig. 2. It can be found that a series of fringes will arise simultaneously and form an amplitude-enhanced fringe at the multifrequency case. The amplitude of such a fringe depends on the quantities (or probabilities) of atoms able to be detected at the excited state. Considering that the transverse-velocity distribution is a Gaussian profile, the amplitudes of the $\pm q$ th pair of Ramsey fringes for the case of

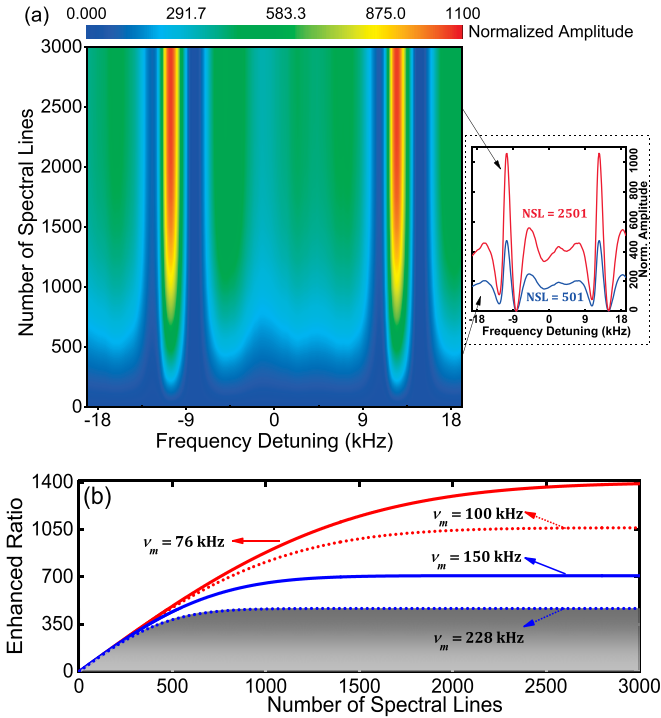


FIG. 3. Characteristics of velocity-grating Ramsey fringes. (a) Line shape of the spectroscopy varied with the Δ and the NSLs. The insets are the normalized spectroscopy when NSLs = 2501 (upper red line) and NSLs = 501 (lower blue line). (b) Amplitude-enhanced ratio \mathcal{R} of the fringes (one recoil part) vs the NSLs and ν_m .

a multifrequency interrogation laser are calculated to be

$$L'_{\text{Ram}} \propto \sum_{n=-\alpha}^{\alpha} \exp \left[- \left(\frac{\Delta + n\omega_m}{0.6\delta\omega_D} \right)^2 \right] \times \text{Re} \{ K e^{i[2(\Delta \pm \delta \mp q\omega_m/2)T + \phi]} \}, \quad (4)$$

where $\alpha = (j - q/2)$ and α can be a half integer, and $\delta\omega_D$ is the Doppler width of the atomic beam. Through numerical calculations (the phase difference ϕ is regarded as a constant during these calculations [29,37]) and integration on the transverse and longitudinal velocities of atoms, the normalized amplitudes of the central two Ramsey fringes (i.e., $q = 0$) varied with the NSLs and the Δ when $\nu_m = 100$ kHz are given in Fig. 3(a). Specifically, the accumulated fringes are shown in the inset of Fig. 3(a) when NSLs = 501 and 2501. Considering the influence of ν_m , the results of the maximum normalized amplitude of the fringes varied with ν_m and the NSLs are given, as depicted in Fig. 3(b). The maximum value of the amplitude-enhanced ratio \mathcal{R} saturates with increasing NSLs and decreases with increasing ν_m . It is obvious that a smaller modulation frequency and larger Doppler width are beneficial to improve the \mathcal{R} . However, an overly small modulation frequency will lead to crosstalk between two adjacent classes of transverse-velocity atoms and thus disturb the atomic coherence. Such an effect can be almost eliminated when the modulation frequency ν_m is larger than 228 kHz which is related to the interrogation time. Notwithstanding, an appropriate ν_m should be chosen to make the trade-off

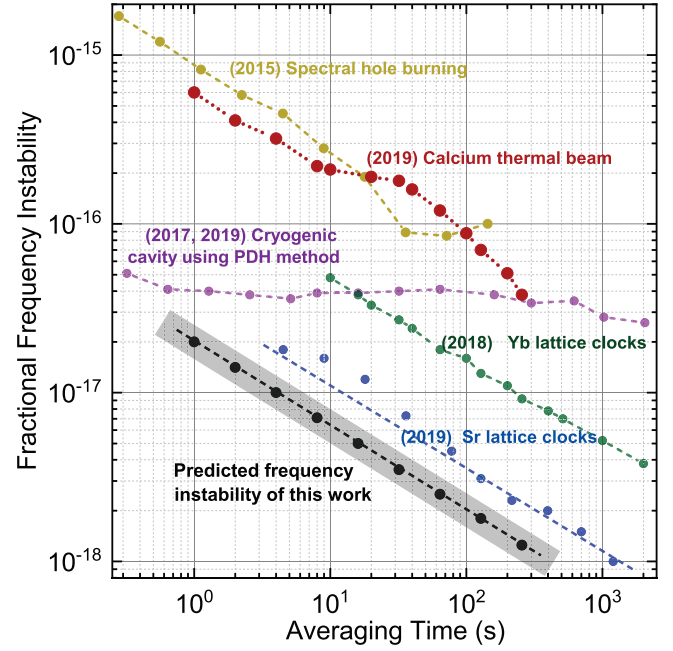


FIG. 4. Fractional frequency instability of this work compared with other works [7,8,16,19,25]. The predicted frequency instability of this work is denoted by the gray dashed line with an asymptote of $2.1 \times 10^{-17}/\sqrt{\tau}$, and the shadow represents the distribution of the frequency instability at different ν_m .

between crosstalk effects and the enhanced ratio \mathcal{R} which desires a small ν_m . When $\nu_m = 100$ kHz, the maximum \mathcal{R} is 1064. But such a value is unrealistic in the traditional method only relying on the increasing of atomic flux, i.e., oven temperature, because a nearly 300 K higher oven temperature is needed.

Due to a substantial improvement in the quantities of the atoms contributing to the Ramsey fringes based on the proposed method, the S/N of the Ramsey fringes can be enhanced by a factor of $\sqrt{\mathcal{R}}$. Therefore, the frequency stability of the laser would be enormously improved. According to the results shown in Fig. 3(b), when the Doppler width is 100 MHz and the linewidth of the Ramsey fringe is ~ 2.0 kHz, the maximum \mathcal{R} of the Ramsey fringes varies from 530 to 1370 at different ν_m ; therefore, the S/N is inferred to be improved by a factor ranging from 23 to 37, and the QPN-limited frequency instability at 1 s can reach a value between 2.6×10^{-17} and 1.6×10^{-17} on the basis of the experimental results in Refs. [25,29].

For a laser stabilization system, the limitations deteriorating the frequency stability typically include QPN and technical noise [38]. Considering that continuous efforts [4,8,16,17,38] are aimed at reaching the QPN, the thermal systems are similarly assumed to be not limited by the technical noise eventually. In other words, only if the technical noise is assumed to be negligible or overcome, does the frequency instability potentially reach the standard quantum limit, which is the 10^{-18} level in short timescales presented in this work. A comparison of the potential fractional frequency instability of this work with that of other laser stabilization systems [7,8,16,19,25,38] is given in Fig. 4. It can be seen that the

predicted QPN-limited frequency instability of this work is even comparable with the best-reported atomic clock [8]. Further improvements on the frequency stability (i.e., S/N) can be realized by increasing the atomic flux, e.g., by properly increasing the oven temperature.

In summary, a velocity-grating Ramsey-Bordé atom interferometry has been proposed herein, in which numerous nonzero-transverse-velocity atoms can now be interrogated and make accumulated contributions to the optical Ramsey fringes. The results show that the amplitude of the optical Ramsey fringes for a thermal calcium beam can be enhanced by more than 1000-fold compared to the traditional

scheme. When applied to laser stabilization, a QPN-limited fractional frequency instability is estimated to be less than $2 \times 10^{-17}/\sqrt{\tau}$, which is comparable with the best-reported optical clocks in short timescales. Such a simple system with superb frequency stability is promising for a wide range of applications besides being used as an optical flywheel in next-generation optical timescales [9,25].

We thank Wei Zhuang for helpful discussions. The work was supported by National Natural Science Foundation of China (NSFC) (91436210) and the National Key Research and Development Program of China.

-
- [1] B. P. Abbott, R. Abbott, T. D. Abbott, M. R. Abernathy, F. Acernese, K. Ackley, C. Adams, T. Adams, P. Addresso, R. X. Adhikari *et al.* (LIGO Scientific and Virgo Collaborations), *Phys. Rev. Lett.* **116**, 061102 (2016).
- [2] T. M. Fortier, M. S. Kirchner, F. Quinlan, J. Taylor, J. C. Bergquist, T. Rosenband, N. Lemke, A. Ludlow, Y. Jiang, C. W. Oates *et al.*, *Nat. Photonics* **5**, 425 (2011).
- [3] X. Xie, R. Bouchand, D. Nicolodi, M. Giunta, W. Hänsel, M. Lezius, A. Joshi, S. Datta, C. Alexandre, M. Lours *et al.*, *Nat. Photonics* **11**, 44 (2017).
- [4] A. D. Ludlow, M. M. Boyd, J. Ye, E. Peik, and P. O. Schmidt, *Rev. Mod. Phys.* **87**, 637 (2015).
- [5] Y. Huang, H. Guan, P. Liu, W. Bian, L. Ma, K. Liang, T. Li, and K. Gao, *Phys. Rev. Lett.* **116**, 013001 (2016).
- [6] Boulder Atomic Clock Optical Network (BACON) Collaboration, *Nature (London)* **591**, 564 (2021).
- [7] W. F. McGrew, X. Zhang, R. J. Fasano, S. A. Schäffer, K. Beloy, D. Nicolodi, R. C. Brown, N. Hinkley, G. Milani, M. Schioppo *et al.*, *Nature (London)* **564**, 87 (2018).
- [8] E. Oelker, R. B. Hutson, C. J. Kennedy, L. Sonderhouse, T. Bothwell, A. Goban, D. Kedar, C. Sanner, J. M. Robinson, G. E. Marti *et al.*, *Nat. Photonics* **13**, 714 (2019).
- [9] W. R. Milner, J. M. Robinson, C. J. Kennedy, T. Bothwell, D. Kedar, D. G. Matei, T. Legero, U. Sterr, F. Riehle, H. Leopardi, T. M. Fortier, J. A. Sherman, J. Levine, J. Yao, J. Ye, and E. Oelker, *Phys. Rev. Lett.* **123**, 173201 (2019).
- [10] T. Nakamura, J. D. Rodriguez, H. Leopardi, J. A. Sherman, T. M. Fortier, X. Xie, J. C. Campbell, W. F. McGrew, X. Zhang, Y. S. Hassan *et al.*, *Science* **368**, 889 (2020).
- [11] N. Ashby, T. E. Parker, and B. R. Patla, *Nat. Phys.* **14**, 822 (2018).
- [12] M. Takamoto, I. Ushijima, N. Ohmae, T. Yahagi, K. Kokado, H. Shinkai, and H. Katori, *Nat. Photonics* **14**, 411 (2020).
- [13] C. Lisdat, G. Grosche, N. Quintin, C. Shi, S. M. F. Raupach, C. Grebing, D. Nicolodi, F. Stefani, A. Al-Masoudi, S. Dörscher *et al.*, *Nat. Commun.* **7**, 12443 (2016).
- [14] T. Takano, M. Takamoto, I. Ushijima, N. Ohmae, T. Akatsuka, A. Yamaguchi, Y. Kuroishi, H. Munekane, B. Miyahara, and H. Katori, *Nat. Photonics* **10**, 662 (2016).
- [15] F. Riehle, *Nat. Photonics* **11**, 25 (2017).
- [16] D. G. Matei, T. Legero, S. Hafner, C. Grebing, R. Weyrich, W. Zhang, L. Sonderhouse, J. M. Robinson, J. Ye, F. Riehle, and U. Sterr, *Phys. Rev. Lett.* **118**, 263202 (2017).
- [17] W. Zhang, J. M. Robinson, L. Sonderhouse, E. Oelker, C. Benko, J. L. Hall, T. Legero, D. G. Matei, F. Riehle, U. Sterr, and J. Ye, *Phys. Rev. Lett.* **119**, 243601 (2017).
- [18] J. M. Robinson, E. Oelker, W. R. Milner, W. Zhang, T. Legero, D. G. Matei, F. Riehle, U. Sterr, and J. Ye, *Optica* **6**, 240 (2019).
- [19] S. Cook, T. Rosenband, and D. R. Leibrandt, *Phys. Rev. Lett.* **114**, 253902 (2015).
- [20] D. Yu and J. Chen, *Phys. Rev. Lett.* **98**, 050801 (2007).
- [21] J. Chen, *Chinese Science Bulletin* **54**, 348 (2009).
- [22] D. Meiser, J. Ye, D. R. Carlson, and M. J. Holland, *Phys. Rev. Lett.* **102**, 163601 (2009).
- [23] M. A. Norcia, J. R. K. Cline, J. A. Muniz, J. M. Robinson, R. B. Hutson, A. Goban, G. E. Marti, J. Ye, and J. K. Thompson, *Phys. Rev. X* **8**, 021036 (2018).
- [24] S. A. Schäffer, M. Tang, M. R. Henriksen, A. A. Jorgensen, B. T. R. Christensen, and J. W. Thomsen, *Phys. Rev. A* **101**, 013819 (2020).
- [25] J. Olson, R. W. Fox, T. M. Fortier, T. F. Sheerin, R. C. Brown, H. Leopardi, R. E. Stoner, C. W. Oates, and A. D. Ludlow, *Phys. Rev. Lett.* **123**, 073202 (2019).
- [26] Huang Kai-Kai, J. Zhang, D. Yu, Z. Chen, W. Zhuang, and J. Chen, *Chin. Phys. Lett.* **23**, 3198 (2006).
- [27] J. J. McFerran and A. N. Luiten, *J. Opt. Soc. Am. B* **27**, 277 (2010).
- [28] H. Shang, X. Zhang, S. Zhang, D. Pan, H. Chen, and J. Chen, *Opt. Express* **25**, 30459 (2017).
- [29] J. Olson, Ph.D. thesis, University of Colorado, Boulder, 2019.
- [30] J. Träger, *Sov. J. Quantum Electron.* **10**, 1255 (1980).
- [31] F. Riehle, J. Ishikawa, and J. Helmcke, *Phys. Rev. Lett.* **61**, 2092 (1988).
- [32] K. Qu, S. Zhao, X. Li, Z. Zhu, and D. Liang, *IEEE Photonics Technol. Lett.* **29**, 255 (2017).
- [33] R. Wu, V. R. Supradeepa, C. M. Long, D. E. Leaird, and A. M. Weiner, *Opt. Lett.* **35**, 3234 (2010).
- [34] X. Yan, X. Zou, W. Pan, L. Yan, and J. Azaña, *Opt. Lett.* **43**, 283 (2018).
- [35] S. Preußler, N. Wenzel, and T. Schneider, *IEEE Photonics J.* **6**, 7901608 (2014).
- [36] B. Hemingway, T. G. Akin, S. Peil, and J. V. Porto, *Phys. Rev. A* **101**, 053410 (2020).
- [37] Ch. J. Bordé, Ch. Salomon, S. Avrillier, A. Van Lerberghe, Ch. Bréant, D. Bassi, and G. Scoles, *Phys. Rev. A* **30**, 1836 (1984).
- [38] M. Schioppo, R. C. Brown, W. F. McGrew, N. Hinkley, R. J. Fasano, K. Beloy, T. H. Yoon, G. Milani, D. Nicolodi, J. A. Sherman, N. B. Phillips, C. W. Oates, and A. D. Ludlow, *Nat. Photonics* **11**, 48 (2017).